On the Rotation of Post-T Tauri Stars in Associations

Ramiro de la Reza[1] and Giovanni Pinzón[2]

Observatório Nacional, Rio de Janeiro, Brazil

ABSTRACT

Nearby associations or moving groups of post-T Tauri stars with ages between $\sim$10 and 30 Myr are excellent objects for the study of the initial spin up phase during the pre-main sequence evolution. An empirical approach is adopted here for the first time with these stars to infer their rotations properties and relations to X-ray emission. Three nearby associations with distances less than 100 pc are considered. The TW Hya association (TWA) with an age of 8 Myr, the Beta Pictoris moving group (BPMG) with an age of 12 Myr and a combination of Tucana and Horologium associations Tuc/HorA (30 Myr). Two low and high rotation modes are considered for each association with stellar masses of $0.1 \leq M < 1.5$ $M_\odot$ and $1.5 \leq M \leq 2.6$ $M_\odot$ respectively. Because no observed rotational periods are known for these stars, we use a mathematical tool to infer representative equatorial rotation velocities $v_0(eq)$ from the observed distribution of projected rotational velocities (*vsini*). This is done for each mode and for each association. A spin up is found for the high rotation mode, whereas in the low rotation mode the $v_0(eq)$ do not increase significantly. This insufficient increase of $v_0(eq)$ is probably the cause of a decrease of the total mean specific angular momentum for the low mass stars between 8 and 30 Myr. However, for the high mass stars, where a sufficient spin up is present, the specific angular momentum is practically conserved in this same time interval. A two dimensional (mass and *vsini*) K-S statistical test yields results compatible with an spin up scenario. By supposing that the distribution of masses of these three associations follows a universal mass function, we estimate the number of members of these associations that remain to be detected. The analysis of rotation and stellar masses using the luminosity X-rays indicators L_x and L_x/L_b present similar properties, as the dependence on

---

[1]delareza@on.br

[2]gpinzon@on.br

stellar mass and rotation, at least for the younger associations TWA and BPMG, to those obtained for T Tauri stars in the Orion Nebula Cluster (1 Myr). A strong desaturation effect appears at ∼30 Myr, the age of Tuc/HorA, measured essentially by the early G and late type F stars. This effect seems to be provoked by the minimum configuration of the stellar convection layers, attained for the first time for the higher mass stars at ∼30 Myr. The desaturation appears to be independent of rotation at this stage.

Subject headings: open clusters and associations: individual (TW Hydrae, βPictoris, Tucana, Horologium) - stars: pre-main sequence, -stars: rotation, X-rays: stars

1. Introduction

Studies of the rotational evolution of pre-main sequence (PMS) stars, from the initial stage of T Tauri stars (TTS) up to the arrival to the main sequence (MS), are mainly devoted to angular momentum transfer processes, X-ray emissions and on possible actions of dynamo mechanisms. Due to the recent use of wide field CCD image applied to dense PMS clusters, a spectacular increase of measured photometric rotation periods with very high accuracy has taken place in the literature. Also, the use of ROSAT and especially CHANDRA X-ray satellites enabled the measurement of hundreds of PMS in the Orion Nebula Cluster (ONC) with an age of 1 - 3 Myr (Feigelson et al. 2003, Flaccomio et al. 20003a, Stassun et al. 2004).

Several challenging problems, such as the existence or not of a bimodal rotation for stellar masses greater than $0.4M_\odot$ in the ONC (Herbst et al.2001, Rebull et al.2001), have been discussed recently in the literature. The reality of these modes in ONC could be related to the action of a magnetic braking mechanism between the star and the surrounding accreting disks. In this sense several studies directed their efforts to study large samples in the ONC and other similar young clusters. Nevertheless, Stassun et al. (1999) found no evidence for a dominant magnetic disk locking in ONC. Rebull et al.(2004) proposes the necessity of even larger samples in order to obtain a clear statistical correlation between rotation periods and disks. Another problem is the presence of rapid low mass (≤ 0.6 $M_\odot$) rotators in the relative older cluster of the Pleiades (∼100 Myr) (Barnes, Sofia & Pinsonneault 2001). Stassun et al. (1999) showed that the distribution of the projected rotational velocities (*vsini*) of Pleiades stars is similar to that of the ONC, indicating that what exists, in this case at 100 Myr, was already established in the first 1 Myr (see also Mathieu 2003).

In general, these problems seem to be related to the different lifetimes of the accreting disks (Tinker et al. 2002). In view of this, it appears that studies of stellar rotation in the *age - gaps* between 1 and 100 Myr (Stassun & Terndrup 2003) are necessary and will probably shed more light on these matters and also on the problem of up to when the angular momentum is conserved or not (Wolff, Strom & Hillenbrand 2004). By considering in this work post-T Tauri stars (PTTS) with ages between 8 and 30 Myr, we try to fill these gaps and also to put into evidence some of the initial speed up processes of stars (Bouvier, Forestini & Allain 1997; Siess & Livio 1997) which could begin to occur at ∼10 Myr (Rebull et al. 2004). This speed up is possible, because PTTS, apart some very few exceptions, are devoided of TTS types of disks. These stars are then free to increase their rotations following a normal evolutionary process.

Concerning the more evolved PTTS with ages ≥ 5 Myr up to near 40 Myr, measured periods are scarce. One of the reasons for this absence, is the inherent difficulty in measuring these stars which, because of their proximity (≤ 100 pc), are distributed in vast areas of the sky. However, some photometric periods have been obtained, for 34 PTTS in Lupus (Wichmann et al. 1998), with a mixture of ages between near 10 and 37 My and also for 9 PTTS belonging to visual binaries Lindroos systems where the primary is a late B star (Huélamo 2002). In addition, a large mixture of ages is also here present.

Even if PTTS can be generally defined as low mass stars with ages between 10 and 100 Myr (Jensen 2001), it is not clear what are the real limits in both extremes. The purpose of this work is to introduce, for the first time as far as we know, a general study of rotation of PTTS belonging to coeval nearby associations of ages between ∼10 and ∼30 Myr. Contrary to the PTTS mentioned before, these stars belong to moving groups having definite ages. We believe that the use of discrete ages systems will introduce a fine-tuning and a more clear picture of the evolution of PTTS in this interval of ages. To do this, we use the following nearby associations: TWA, BPMG and Tuc/HorA. The ages of these groups have been determined by using a Hertzsprung-Russel (HR) diagram, but in some cases a completely different and independent method, based on the confinement of past 3D Galactic orbits, produced similar results confirming these ages. This is the case of BPMG where the here adopted HR age of 12 Myr (Zuckerman et al. 2001a) is consistent with that obtained kinematically (Ortega et al. 2002, 2004). For TWA, proposed and used ages based on the HR method range between 5 and 10 Myr (see for instance, Webb et al.1999, Luhman (2001), Torres et al.2003, Weinberger at al.2004). Here, we adopt for TWA the age of 8 Myr based on recent results obtained kinematically (de la Reza et al.2004 to be submitted). For Tuc/HorA we adopt the age of 30 Myr, which was independently found to be near 30 Myr by the HR method by Torres et al. (2000) for the Horologium Association and by Zuckerman et al. (2001b) for the Tucana Association.

Unfortunately, no measurements of periods for individual members of PTTS associations are presently available, but only their projected ($vsini$) rotation velocities. Because of this, we present here a method to derive representative equatorial velocities $v_0(eq)$ from the $vsini$ data in order to estimate mean periods.

The organization of this paper is the following: In Section 2 we derive the masses and radii and compile a general table containing the main parameters of all members of the associations that will be used in this work. In Section 3 we describe the method to derive the equatorial rotation velocities from $vsini$ data. In Section 4 this method is applied for the three associations under study. In Section 5 we discuss some statistical considerations. Section 6 is devoted to the related X-ray radiation relations and finally the Section 7 contains a summary and our conclusions.

2. Stellar masses and radii

Unfortunately, at present, a fundamental calibration of PMS evolution tracks is lacking. Some of the reasons for this are to be found in the absence of a large sample of model independent mass determinations. Hillenbrand & White (2004) have recently made a careful analysis of masses derived for PMS and MS stars by means a complete set of models and their confrontation with available measured orbital dynamic data for PMS and early MS stars with masses up to $2.0 M_\odot$. Consistency appears, in general, to be better for MS stars above $1.2 M_\odot$. However, for masses below the solar one, PMS models systematically underestimate the masses by 10% to 30%, especially below $0.5 M_\odot$. There are nevertheless, no dynamical PMS constraints for masses below $0.3 M_\odot$.

Concerning the PMS stars in associations, the situation is worst because in general no mass values have been published. In these circumstances and as the models give in general similar results we have chosen only one model (Siess, Dufour & Forestini 2000) to obtain the masses and radii of all the members of the considered associations at their respective ages. This has been done for masses comprised between 0.1 and $2.5 M_\odot$ using available observed photometric data of the individual members. Following the recommendation of Stauffer (2001) we use, whenever possible, $(V - I_c)$ colors and when this is not the case, $(B - V)$ colors.

All stellar masses and radii derived this way are listed in Tables 1,2 and 3 together with their observed photometric colors. Some considerations about the completeness of the members of these associations will be made in Section 5.

3. The Stellar Rotation

3.1. Determination of mean equatorial velocities

The distribution of projected *vsini* rotational velocities $\phi(vsini) = \phi(y)$ is related to the true rotational velocities distribution $f(v)$, considered here to be the equatorial velocities $v_0(eq)$, through an integral equation (Chandrasekhar & Munch 1950). Assuming that the rotation axes are randomly distributed in space, this relation is

$$\phi(y) = y \int_y^\infty \frac{f(v)dv}{v\sqrt{v^2 - y^2}} \tag{1}$$

It is not an easy task to derive $f(v)$ from $\phi(y)$ by a numerical inversion procedure (Gaigé 1993) because $\phi(y)$ has to be differenciated. For this, it is necessary that the observed distribution $\phi(vsini)$ (normally in histograms) be transformed into a continuous function. This is possible when we have at our disposing a large collection of good quality *vsini* data. The inversion has been realized for the Pleiades young cluster (age 70-125 Myrs) using *vsini* data for 235 members stars (Queloz et al. 1998). Differently from young clusters, where in general more than one hundred stars can be measured, the PTTS associations contain much less members. This is the case of TWA and BPMG each of which possesses near 30 members with a large proportion of visual binaries in the case of TWA. Adding all probable and possible members of Hor and Tuc A (where much less binaries are present) we obtain a total of about 50 objects.

Due to the relative low number of PTTS in associations and also considering the uncertainties in *vsini* values between 2 and 5 $km\ s^{-1}$ (in the best case) for low and high rotators respectively, a different strategy must be followed. We follow here the suggestion of Chandrasekhar and Munch (1950) for the case of few data which consists of assuming a parametric form of $f(v)$ instead of inverting the integral equation (1). We can then compute the integral in (1) and obtain the corresponding $\phi(vsini)$ distribution which will be compared to the observational distribution of *vsini* for each association.

Different functions, from a simple rectangular to a more elaborated parabolic representation were tested by Brown (1950) and give, so as the gaussian used by Chandrasekhar and Munch, fairly similar results. We then use this rectangular function as proposed by Brown by taking $f(v)dv$, the probability of ocurrence of v between v and $v + dv$, to be equal to $dv/2a$ for $v > v_0 - a$ and $v < v_0 + a$ and equal to zero otherwise. The rectangle centered at the probable velocity v_0 has a height of $1/2a$ and a total width of $2a$. To compare with observations, a cumulative distribution function of the projected velocities is defined

as $\Phi(y) = \int \phi(y)dy$. The integration is realized over finite intervals of y corresponding to the grouping of the observations. The fraction of stars with $(vsini)_l < y < (vsini)_{l+1}$ is given by $\Phi(vsini)_{l+1} - \Phi(vsini)_l$. Multiplying this difference by the total number of stars in the association we obtain the total number of stars in that interval of $vsini$ values. The resulting cumulative function $\Phi(y)$ is a monotonically increasing function from zero to one as y increases. To calculate $\Phi(y)$ we used the relation (6) of Brown (1950). The derivative of $\Phi(y)$ using one hundred successive intervals of y will finally be compared with the observed $\phi(vsini)$ distributions.

4. Observed rotation data

The start point of our analysis will be stellar masses, more properly we will choose *a priori* a specific mass value in the interval 0.1-2.6$M_\odot$ separating low mass (LM) and high mass (HM) stars. This mass divisor is chosen by considering the *vsini* distribution as presented in Figures 4 and 5.

An examination of the points in the (*vsini*, mass) plane of these two figures permits to distinguish that a different pattern of *vsini* values appears at $\sim 1.5 M_\odot$. Because of this, we call LM stars those with masses smaller than $1.5 M_\odot$ and HM stars, those with masses larger or equal than $1.5 M_\odot$. The corresponding low mode (LRM) contains, in general, low *vsini* values (note however, that Tuc/HorA contain some LM stars with high *vsini* values). The high rotation mode (HRM) contains higher *vsini* values as compared to the low ones. As will be seen in section 5, this choice of mass separation finds a statistical justification. Anyway, we expect that the physical importance resulting from the above separation of stellar masses will emerge in this work.

4.1. The Spin up and the specific angular momentum behavior

In Figure 1 we present six histograms containing the distributions of the observed *vsini* values for the LRM and HRM and for the three considered associations. The dashed line curves in some of these histograms represent the best fit of the frequency distributions. For the LRM they correspond to mean equatorial velocities $v_0(eq)$ of 28±5, 25±5 and 32±5 kms^{-1} respectively for TWA, BPMG and Tuc/HorA. For the HRM we were able to adjust a curve only for the case of Tuc/HorA where a small peak appears to emerge. Due to the nature of the HRM *vsini* distribution of the HRM of TWA (where only two HM stars have been detected until now) and BPMG, our fitting procedure does not apply. Nevertheless,

quite good representative $v_0(eq)$ values can be obtained by multiplying average $vsini$ value by the factor $4/\pi$ (Chandrasekhar & Munch 1950).

In these conditions, the resulting HRM $v_0(eq)$ values for TWA, BPMG and Tuc/HorA are respectively equal to 113, 139 and 159±5 kms^{-1}. All $v_0(eq)$ values are indicated in Figure 1 and in Table 4. Considering the successive ages of these associations, a mean spin up appears to be present for the HRM, whereas the $v_0(eq)$ in LRM are not so different. This behavior agrees with the known slow stellar evolution of LM stars contrary to HM stars, where the evolution is faster. Future measured periods of individual star members of these associations, will probably allow to confirm these results. In any case, we found a continous spin up behavior up to 30 Myr which is near the 40 Myr maximum spin up found in PMS models (Siess & Livio 1997). If this is the case, HM stars could be used as gyrochronometers following the spin pattern of different associations. A new tool would then be at hand to estimate the age of an association by examining their high mass content.

By estimating a mean radius $< R >$ and using the $v_0(eq)$ mentioned above for these associations we can determine mean rotation periods as we will see later, but for the moment we can estimate the behavior of the specific mean angular momentum $J/M = k_{tot}^2 \times v_0(eq) \times < R >$, where k_{tot} is the total radius of gyration. Depending on the mass and on the age, the values of k_{tot}^2 consider the changes of the stellar moment of inertia, specially the receding of the convective zone leaving more centrally condensed stars. Here, we have used the k values for convection and radiation furnished by the PMS models of Siess et al.(2000). The ensemble of k^2 values and the resulting J/M values in $cm^2 s^{-1}$ for the representative $v_0(eq)$ and $< M >$ are presented in Table 4. Taking into account the adverse effects of an unequal mass distributions of these associations, the fact that only two HM stars are present in TWA, and the dominant large radii estimated in BPMG (see Table 2), we found that a mean decrease of factor two is present for low mass stars between ~10 and 30 Myr. Some undetected mechanisms is active in the low mass stars dissipating angular momentum and preventing these stars from having sufficiently larger surface velocities in order to conserve their J/M. On the other hand, the high mass stars develop a sufficient spin up that practically mantains a conserved J/M in this same time interval. Also, with the exception of the LRM comparison between TWA and BPMG, the other three possible comparisons between the modes and associations of different ages show that $< R >$ decreases as $\propto t^{-1/5}$.

5. A statistical approach

In Section 4 by means of the observed $vsini$ distribution we found, for the three associations, mean representative equatorial rotation velocities for two different types of stellar

masses. Also we found that a clear spin up is present, at least for the considered high mass stars between 8 and 30 Myr (see Table 4). In this section we explore the completeness of our data members and perform a statistical treatment of the mass and *vsini* data in order to examine the consistency with the observed spin up process.

5.1. Initial Mass Functions

The number of members of the associations collected in Tables 1, 2 and 3 is not intended to be complete. We have selected from the literature all probable and possible members, although is quite possible that future investigations could eliminate some of these members. On the other hand, several members depending on their masses, remain to be detected. In order to estimate the number of stars that probably could be discovered, we assume that the mass spectrum follows an universal mass distribution. We do so, even considering that the formation of these groups could be triggered by a mechanism, different from those of young clusters related mainly to gravitational processes. In fact, as shown in Ortega et al (2002, 2004), BPMG was probably formed $\sim$12 Myr ago by the impact pressure of a supernova front shock originated in the OB association Sco-Cen. This appears also to be the case, for TWA $\sim$8 Myr ago (de la Reza et al. 2004, to be submitted).

In this discussion we consider only stars with masses between 0.1 and $2.6 M_\odot$ that we obtain in these associations. We do not discuss, or take into account, the few brown dwarfs stars with masses less than $0.1 M_\odot$ that have been detected among these groups. This is the case of TWA 5B, GSC 8047-0232B and HR7329B (see for instance Neuhäuser & Guenther 2004). Also, visual binaries (TWA is full of them!) are considered as simple stars for mass distribution purposes.

As a convenient *universal* initial mass function (IMF) we choose the one proposed by Scalo (1998) (see below), but before adjusting it to the data we have to take into consideration that the observed mass distributions in the associations are slightly different. While, TWA appears to be well fitted in the range of very low mass stars $(0.1\text{-}0.25) M_\odot$, this is not the case for BPMG and Tuc/HorA. On the contrary, higher masses appears to be better represented in BPMG, Tuc/HorA than in TWA. This last group has only two stars in our defined high mass regime.

Here, we assume that TWA is complete in the very low mass range. We can then fit the height of Scalo distribution with this group. The adopted Scalo (1998) distribution is the following:

$$\xi(m) = k \left\{ \begin{array}{ll} D_0 m^{D_1} & if \quad 0.1 \leq m/M_\odot \leq 1.0 \\ D_0 m^{D_2} & if \quad 1.0 \leq m/M_\odot \leq 2.6 \end{array} \right\} \tag{2}$$

where k is an adjusting constant, D_1 and D_2 correspond to the slope of logarithmic IMF at each mass interval and $D_0 = 32$ is a constant involving the age of the Galactic disc (Miller & Scalo 1979). Analytic fits to the IMF using only two parts of the three-segment power law given by Scalo (1998) give: $D_1 = -0.2 \pm 0.5$ and $D_2 = -1.7 \pm 0.5$, corresponding to the mass interval 0.1-10$M_\odot$. We have obtained the best fit to the observations by adopting $D_1 = 0.1$ and $D_2 = -1.4$. In Figure 2 we show the result of this fit for the three associations and for which we have adopted a general bin of 0.5$M_\odot$.

The number of stars that remain to be discovered for each association, if they follows the IMF, can be estimated by the difference of the number of stars between the IMF and the observed distributions. These are shown in Figure 2. A first tentative to estimate the number of high mass stars of TWA by a IMF approach was made by (Webb 2001).

5.2. *vsini* distribution with age

Having of a number of observed stars with their respective masses and *vsini* values and using also the number of the remaining stars to be detected, we can try to complete the observed histograms presented in Figure 1. For this we must simulate *vsini* values for these remaining stars. This can be done by multiplying the mean $v_0(eq)$ values obtained from observational data in Section 3 by random *sini* values (note that this assumption of random distribution of the inclination axes has been made to obtain the $v_0(eq)$ values). Several tests of random *sini* between 0 and 1 produced similar results because they are conditioned by the used $v_0(eq)$ values. A typical result is shown in Figure 3. We notice that the distribution of observed and simulated values of *vsini* is compatible with a spin up process in the interval of ages. We should note that we cannot use the evolution of this distribution to extrapolate to younger and older ages to obtain a ressemblance of the *vsini* distribution as is the case for comparison between the distribution of *vsini* in ONC and the Pleiades done by (Stasssun et al.1999, see also Mathieu et al.2003). This is because these associations do not appear to contain very high rotators with masses below 0.6$M_\odot$ as in the case of the Pleiades. Nevertheless, some observed low mass with very high *vsini* values exist in Tuc/HorA for masses between 0.7 and 1.0$M_\odot$ (see Figure 5). Also, our determination of mean equatorial velocities is not capable to properly consider these few stars.

5.3. A two dimensional K-S analysis

In order to statistically quantify the observed distribution of *vsini* for low and high mass stars between two associations with different ages we use a Kolmogorov-Smirnov analysis (K-S). While the standard one dimension K-S test does not appear to produce significative measurable differences, with the exception of the obvious case of HRM between TWA and BPMG, a two dimensional K-S test appears to be more interesting to visualize the spin up process.

Differently from the traditional one dimension K-S test, where a simple value can represent the maximum difference between two cumulative distributions, the two dimensional K-S test use a relative different approach. This is due to the fact that a cumulative two dimensional distribution is not defined. Following Press et al. (1994) the discriminator must then be viewed in one quadrant of the four containing all the points in a two dimensional distribution.

The two dimensions chosen here are the stellar mass and the observed *vsini* values as shown in Figures 4 and 5 for the TWA-BPMG and BPMG-Tuc/HorA comparison respectively. For the two dimensional K-S test we apply the mathematical recipe presented in Press et al. (1994).

When the populations of two associations of different ages are compared in the same plane, the program evaluate, for each population an origin point of the four quadrants. In principle one of the four quadrants will show the largest differences between the distribution of points. These differences can then be quantified in the following manner: in each quadrant the number of points of each population is counted and divided by the total number of points of each population (without considering the origin point). For each quadrant these two predictions are subtracted. The quadrant that presents the largest difference is the one indicating the largest differences in the points distribution.

In Figure 4 for instance we present the results of the comparison of TWA (triangles) and BPMG (squares). Each one producing a system of four quadrants. We represented here only the case centered on BPMG stars (that based on TWA stars, and not showed here, produces similar results). In each quadrant the difference of their corresponding ratios one with respect to the other is shown. The upper value for the TWA-BPMG comparison and the lower one for the BPMG-TWA comparison.

In both cases, we see that the upper right quadrant corresponding to larger masses and higher *vsini* values is that presents the largest different distribution of values. In Figure 5 we show the same type of results for the comparisons between BPMG-Tuc/HorA also indicating the same upper right quadrant for the largest differences.

The axis center is placed at $0.7 M_\odot$ when using the TWA distribution because this group has the largest distributions of low masses. Whereas, due to the relatively more massive distributions in BPMG and Tuc/HorA their center point is at 1.3 $M_\odot$. It is interesting to note that this center is similar to our 1.4 $M_\odot$ value used to discriminate LM and HM stars. This supports, in a certain way, our *a priori* chosen mass divisor value.

We performed similar calculations (not shown here) using the observed and simulated *vsini* values as computed before. The results for the BPMG-Tuc/HorA population comparisons are similar to those using only observed values. The results of the observed plus simulated comparison between TWA and BPMG are however less clear. The upper right quadrant becoming less important and being almost similar to the upper left quadrant. This is due to the largest increase of simulated stars with masses larger than $0.25 M_\odot$ for TWA.

In any case, the two dimensional K-S test for the case of pure observed values is compatible with the presence of a spin-up process dominated by HM stars in these associations.

6. X-rays versus rotation

One of the main purposes of studies of X-ray radiation in PMS stars is the search for correlations with stellar rotation in order to shed some light on the question about what kind of dynamo is into action (see Feigelson et al. 2003 for a discussion on different dynamo mechanisms). Before presenting our results concerning the X-rays properties in PTTS for ages between 8 and 30 Myr we present here the results obtained for ONC ($\sim$1 Myr) in order to see for possible connections among these ages.

Three main recent studies in ONC, based on hundreds of X-rays measurements obtained with CHANDRA, deserve particular consideration. Feigelson et al.2003 and Flaccomio et al.2003a found in ONC that stars with measured periods are near the saturated regime at $logL_x/L_b =\sim$-3. (-3 is the canonical saturation value of the linear MS relation shown in Figure 6 and L_b is the bolometric luminosity). However, the mean $logL_x/L_b$ values of Feigelson et al. (shown in Figure 6) present values smaller than -3, suggesting more a super-saturated regime. Concerning the relations of these fluxes with rotation and differently from Flaccomio et al. which do not find any apparent rotation/X-ray relationship, Feigelson et al. does find a slight mean relation with rotation periods, in an inverse way as that of the MS linear relation. As can be seen in Figure 6, the Feigelson et al. data appears to show lower $logL_x/L_b$ values for high rotators. In a recent work Stassun et al.(2004) re-analyses all the ONC data, this time including also those stars with no measurable rotation periods. The main recent results of Stassun et al., which can be compared with those of Feigelson

et al. and Flaccomio et al. are the following: 1) most stars with measured rotation periods (more X-ray luminous in general) are placed in the super- saturated regime 2) the relation with rotation is confirmed in the sense that high rotations indicate lower L_x/L_b values 3) as also found by Feigelson et al. and Flaccomio et al., L_x increases with the stellar mass 4) by finding that stars with accreting signatures present lower X-ray luminosities, probably resulting from absorption by the circumstellar disks, they confirm the Flaccomio et al. results that the non accreting stars have much larger X-ray luminosities than the accreting ones. 5) an emerging linear MS relation can be present in stars with no observable rotation periods.

There is then a general indication that central stars, and not the disks, are the main source of X-rays. We have chosen also to explore the luminosity L_x and the ratio L_x/L_b, as the main X-rays indicators for the PTTS associations. All these values are taken from ROSAT measurements when available. We prefer to use, as far as possible, published L_x and L_x/L_b values. When this is not the case, we calculate these values using published stellar distances of all the members of the associations. These distances were furnished by Hipparcos or by appropiate kinematical and age considerations used to establish these associations (see Tables 1-3). For the calculations of the fluxes we used classical procedures with $F_x = C(8.31 + 5.30 \times HR1) \times 10^{-12}$, where C is the ROSAT counting rate and $HR1$ the hardness ratio (Jensen 1998) and with $F_b = 2.48 \times 10^{-5} \times 2.512 \times^{-(V+BC)}$, where V is the observed visual magnitudes (see Tables 1-3) and BC, the bolometric correction estimated using (Kenyon & Hartmann 1995) tables. Due to ROSAT resolution, when visual binaries are very close (excepting when the companion is an A type star) we divided F_x by 2. All these L_x and L_x/L_b values are shown in Tables 1-3.

In order to ascertain the general behavior of the X-ray radiation with rotation, we estimate representative rotation periods using the $v_0(eq)$ and mean radii discussed in Sections 2 and 4. The values of these periods are shown in Table 4. Also in this table are included the mean L_x and L_x/L_b values for the LRM and HRM for the three associations. A graphic representation of these values is in Figure 6. This figure contains, for comparison purposes as mentioned before, a schematical representation of the X-ray behavior of ONC (Feigelson et al. 2003). They also contain the linear trend corresponding to the (α-ω) dynamo valid for low rotating MS stars. We also consider in Figure 6, the tendency found for 9 PTTS belonging to Lindroos systems by Huélamo (2002). Even if these stars, apparently mimic the (α-ω) dynamo, this trend is not due to this effect, but to an ageing effect. In fact, the upper stars are very young stars whereas the lower ones are older than 50 Myr.

Concerning the behavior of the PTTS of associations in Figures 7 and 8, we can see that the L_x indicator, except for Tuc/HorA, does not present clear changes for the LRM and HRM. Variations are more clearly seen by means of the L_x/L_b indicator. First, we note that,

different from the case of ONC, the LRM in TWA and BPMG present L_x/L_b at the canonical saturated value. Apparently this could be due to the absence of absorption accreting disks in these stars (see later). Nevertheless, as in ONC, we can see the presence of a small desaturation tendency for HRM in BPMG, also in an opposite direction to the linear MS relation. We note nevertheless, that HRM in TWA depends on only one G5 (TWA19A) star. By desaturation we mean a progressively decreasing of the X-ray indicators with respect to the saturated values. We also note that this happens first in the HRM which implies high masses and large $v_0(eq)$ values. The desaturation effect appears clearly later at $\sim$30 Myr, indicated by both X-rays indicators, only for Tuc/HorA. In Figure 7 and 8 we show the variations of these indicators only as a function of age for the two modes. We have also considered in these figures the values presented by Flaccomio et al.(2003b) for TTS with ages between 1 - 7 Myr and MS stars with ages up to 140 Myr. Our data fills well a large part of the gap in the Flaccomio et al. data. Here, we discuss more in detail this desaturation effect. A discussion of the dependence of the X-rays properties on mass can be instructive. In Figure 9 we present L_x versus stellar masses for the three associations showing a similar increasing trend as observed in ONC (see references mentioned above). In Figure 10 are shown the values of L_x/L_b as a function of stellar masses also for the three associations. A relative similar figure can be found in Song et al. (2003,Fig 19) and Song et al. (2004,Fig.1), although in these figures, differently than in our Figure 9, only new proposed members of TWA, BPMG and Tuc/HorA (also included in this work) and colors (B-V) instead of mass are included. From Figure 9 it can be seen that, even if TWA members are concentrated in the region of very low masses, TWA and BPMG have, in general, similar L_x/L_b values independent of mass. A notorious difference appears for the older Tuc/HorA, where stars with masses larger than $\sim$1.1$M_\odot$ (corresponding to stars of types earlier than $\sim$G3) show a steep decline of the L_x/L_b values. This softening X-rays branch is formed by G, F and A stars. Even if the observed F stars are more numerous in Tuc/HorA than in BPMG, F stars in BPMG have larger values of L_x/L_b than the corresponding stars in Tuc/HorA. An age effect is then into action as far as larger masses than 1.1$M_\odot$ is concerned. We must note that increasing masses (and also increasing stellar temperatures) are a measure of the diminishing of the corresponding stellar convecting layers (see for instance Pinsonneault, DePoy & Coffee 2001). Now, what about rotation ?. Examining the descending branch we can see that its beginning (see Table 3) at $log\ (L_x/L_b) \sim$ -4.0, is formed by stars of types $\sim$G3 to F8 with *vsini* values around $\sim$30 kms^{-1}, whereas at the faint values of $\sim$ -5.0 or less, all stars correspond to very high rotators with *vsini* values larger than 100 kms^{-1}. From this, we can infer that at this stage rotation is no more important. It is interesting to note that this desaturation effect at $\sim$30 myr is due to the fact that at this age, which nicely coincides with the age of Tuc/HorA, began the stabilization of the convecting layers, that is, when for these masses they attain for the first time, the minimun configuration (see

for instance Cameron, Campbell & Quaintrell (1995); Keppens, MacGregor & Charbonneau (1995); Siess & Livio (1997)). The convecting layers are then so thin that an increase of rotation is unable to maintain high values of L_x/L_b resulting from a dynamo process.

We note however,in Figure 10 that the two hotter stars of BPMG, with types F2 ($vsini$=155 kms^{-1}) and one A7 ($vsini = 134$ kms^{-1}) present very low values of L_x/L_b, apparently contradicting our mentioned age effect (this also applies to the sole A star of TWA). From this, we conclude that the age effect for the desaturation process is only sensitive for early G and late F stars. Earlier F and A stars will always show low L_x/L_b values independent of age.

We note that in effect, a discussion based on the mass dependence of the X-ray indicators (as in Figure 10) can give a better insight on the physical origins of the X-ray softening than that based on the rotation period (Figure 6). In fact, a discussion based only in Figure 6 would eventually lead us to conclude that the high rotation is the cause of the X-rays softening, which this is not the cause as seen above.

This kind of behavior is in agreement with other recent studies based on the hardness ratio HR1 used as a measure of the L_x radiation (Kastner et al. 2003; Suchkov, Makarov & Voges 2003). Kastner et al. studied the same PTTS associations considered in this work and detected a clear decline of HR1 values for G, F stars of Tuc/HorA relative to BPMG. They also show that HR1 values of the three associations are somewhat smaller than those of younger TTS (see also the predictions made about this in Suchov, Makarov & Voges 2003). Suchov et al. realized an extensive general analysis of X-ray radiation of F type stars measured by Hipparcos. They found that a small group of extreme X-rays radiators ($logL_x > 30.4$) is dominated by young PMS stars. In our case, we found that almost 3 F stars are included in this range in BPMG, whereas only one in Tuc/HorA. In TWA we found that other type of stars, present these extreme larger L_x values as is the case of the K7 TW Hya star.

In conclusion, it appears that the softening of X-ray radiation with age is related to intrinsic stars properties and not to others effects like absorption by surrounding disks as discussed by Kastner et al. (2003). In fact, with the exception of very few stars in TWA, which have classical TTS fine dusty disks, probably in their last stages, as TW Hya (even if this star is observed pole- on) and Hen600A (TWA3A), no more discs of this kind are seen in these associations. Note also, that the protoplanetary disks detected around TWA 11A and around the Beta Pictoris star are of a different nature than those of TTS. On the other hand, recents surveys searching for the presence of warm dust in members of TWA (Weinberger et al.2004) and in BPMG (Weinberger et al.2003) have shown apart some few stars, a general absence of such warm dust. No similar survey has been made around Tuc/HorA stars,

but the known absence of IRAS sources among their members, and considering that IRAS radiation is correlated to the presence of warm dust (Weinberger et al.2004), we can expect a similar absence of fine warm dust in Tuc/HorA.

At this stage we mention that the same behavior of L_x/L_b versus temperature or mass, indicating the existence of a general desaturation effect at this age, is also found in young stellar clusters as IC2602, IC2391 with ages of 30 Myr (Stauffer et al.1997) and NGC 2547 (35 - 54 Myr, Oliveira et al.2003). A similar behavior as our Figure 10 for these three mentioned clusters can be seen in Figure 1 of Jeffries, Totten & James 2000.

How this saturation effect will continue to evolve in direction to the early MS stage? In Figures 7 and 8, we show that the HRM attain the early MS L_x/L_b values at 30 Myr whereas this is not yet the case for the LRM. ROSAT studies of the Pleiades ($\sim$100 Myr) member stars present a different behavior, where low mass stars with $vsini$ values smaller than 10 kms^{-1} have unsaturated L_x/L_b values, whereas stars with larger $vsini$ values exhibit almost constant saturated L_x/L_b values. We believe that studies of other stellar systems with intermediate ages between 30 and $\sim$100 Myr will be helpful to understand these differences, especially considering that angular momentum will not probably be conserved anymore. In general, it is important that rotation periods for individual members of the PTTS associations be observed to confirm our results and that future comparisons with older stars clusters be made as function of rotation $v_0(eq)$ velocities in a mass to mass way.

7. Summary and Conclusions

We have chosen three nearby post-T Tauri stars associations with ages between 8 and 30 Myr (TWA, 8 Myr; BPMG, 12 Myr and Tuc/HorA, 30 Myr) to study the stellar rotations and X-ray related properties. For all probable and possible published members of these associations, we have estimated their model dependent stellar masses and radii by means of their observed $(V - I_c)$ colors. We collected all best observed projected rotational velocities $vsini$ values. When possible, the X-rays indicators L_x and L_x/L_b were taken from the literature. When this was not the case, we calculated the fluxes F_x and F_b by standard methods. All distances used to calculate some luminosities were taken from the literature.

From the distribution of stellar masses versus vsini values we chose *a-priori*, two groups of masses: low mass stars between 0.1 and $1.4M_{\odot}$ and high masses, between 1.5 and $2.6M_{\odot}$. This initial mass division, later justified by a statistical analysis, is fundamental for all the conclusions of this work. Two low and high rotational modes were then established. This first general study of rotation of post-T Tauri stars in associations lead us to the following

conclusions:

Because no measurements of the stellar rotation periods exist for these stars, we inferred, by means of a numerical approach, representative equatorial rotation velocities obtained from the *vsini* observed distribution for each mode and for each association. A spin up was found for the high rotation mode in the whole interval between 8 and 30 Myr which is near the maximum of the spin up found at 40 Myr in pre main sequence stellar models. The spin up is not present in the low mode. In any case, by estimating a mean radius for each association, which in general decreases as $t^{-1/5}$, we found that a mean specific angular momentum is practically conserved during this interval of time for the high mass stars. However, this is not the case for the low mass stars where a decrease of the specific angular momentum by a mean factor two is present. Somehow, these low mass stars do not reach large surface velocities, as is the case of the high mass stars in order to conserve their specific angular momentum.

By admitting that the star's mass distribution in the associations follows an universal initial mass function, we estimated the star's members that remain to be detected for different mass intervals. Simulating *vsini* values for these undetected stars, we showed that their distribution, together with the observed *vsini* values, is in agreement with a general spin up picture. Another result, even more compatible with a spin up of the high rotating mode, is obtained by means of a two dimensional (mass and observed vsini) K-S statistical analysis.

Taking into account the two X-rays indicators; L_x and L_x/L_b, we found that stars, specially in the younger TWA and BPMG associations, present some similar properties to those of T Tauri stars in the Orion Nebula cluster (1 Myr). These are: a direct L_x correlation with mass and a slight dependence with rotation in the sense of falling L_x/L_b for lower rotation periods. This trend is opposite to the linear relation valid for low rotators in the main sequence. A strong desaturation effect appears for the high mode in Tuc/HorA. The nature of this effect is better understood when L_x/L_b is plotted against the stellar masses. This desaturation at 30 Myr is sensitive only for high mass early G and late type F stars. This effect appears to be due only to intrinsic stellar properties. In fact, at ∼30 Myr (which coincides with the age of Tuc/HorA) the stellar convective layers of these high mass stars, attain for the first time their minimum configuration. Because of this, their even very large rotation velocities appear unable to maintain high L_x/L_b values. A similar behavior of L_x/L_b is also found, at the same age, in young clusters as IC2602,IC2391 and NGC2547.

Our results fill the gap of the general variation of the X-rays indicators between T tauri stars and early main sequence stars. Whereas in the low rotation mode the transition appears to be soft, in the high rotation mode the indicators reach, at 30 Myr, nearly the early main sequence values.

REFERENCES

Barnes, S., Sofia, S. & Pinsonneault, M., 2001, AJ, 548, 1071

Bouvier, J., Forestini, M., & Allain, S., 1997, A&A, 326, 1023

Cameron, A.C., Campbell, C.G. & Quaintrell, H., 1995, A&A, 298, 133

Brown, A., 1950, ApJ, 111, 366

Chandrasekhar, S. & Munch, G., 1950, ApJ, 111, 142

Feigelson, E., Gaffney, J., Garmire, G., Hillenbrand, A. & Townsky, L., 2003, ApJ, 584, 911

Flaccomio, E., Micela, G. & Sciortino, S., 2003a, A&A, 402, 277

Flaccomio, E., Micela, G. & Sciortino, S., 2003b, A&A, 397, 611

Gaigé, Y., 1993, A&A, 269, 267

Herbst, W., Bailer-Jones, C.A.L. & Mundt, R., 2001, ApJ, 554, L197

Hillenbrand, L. A. & White, R. J., 2004, ApJ, 604, 741

Huélamo, N., 2002, Ph.D. thesis, Universidad Autónoma de Madrid, Madrid.

Kastner, J. H., Crigger, L., Rich, M. & Weintraub, D., 2003, ApJ, 585, 878

Kenyon, S. J. & Hartmann, L. W., 1995, ApJS, 101, 117

Keppens, R., MacGregor, K. B. & Charbonneau, P., 1995, AJ, 294, 469

Jensen, E. L. N., 2001, in ASP Conf. Ser., Vol. 244, Young Stars Near Earth: Progress and Prospects, ed. R. Jayawardhana & T. Greene(San Francisco: ASP)

Jensen, E. L. N., Cohen, D. H., & Neuhäuser, R. 1998, AJ, 116, 414

Luhman, K.L., 2001, in ASP Conf. Ser., Vol. 244, Young Stars Near Earth: Progress and Prospects, ed. R. Jayawardhana & T. Greene(San Francisco: ASP)

Mathieu, R. D., 2003, in Stellar Rotation, Proc. of the IAU Symp. 215, eds. A. Maeder & P. Eenens

Mamajek, E.E., Meyer, M.R. & Liebert, J. 2002, AJ, 124,1670

Miller, G. E. & Scalo, J., 1979, ApJS, 41, 513

Muzerolle, J., Hillenbrand, L., Calvet, N., Hartmann, L. & Briceño, C. 2001, in ASP Conf. Ser., Vol. 244, Young Stars Near Earth: Progress and Prospects, ed. R. Jayawardhana & T. Greene(San Francisco: ASP)

Ortega, V., de la Reza, R., Jilinski, E. & Bazzanella, B., 2002, ApJ, 575, L750

Ortega, V., de la Reza, R., Jilinski, E. & Bazzanella, B., 2004, ApJ, 609, in press

Pinsonneault, M. H., DePoy, D. L. & Coffee, M., 2001, ApJ, 556, L59

Oliveira, J. M., Jeffries, R. D., Devey, C. R. & Barrado y Navascués, D., Naylor, T., Stauffer, J. R. & Totten, E. J., 2003, MNRAS, 342, 651

Press, W. H., Teukolsky, S. A., Vetterling, W. T. & Flannery, B. P., 1994, Numerical Recipes in C, Cambridge University Press

Queloz, D., Allain, S., Mermilliod, J-C., Bouvier, J. & Mayor, M. 1998, A&A, 335,183

Reid, N., 2003, MNRAS, 342, 837

Rebull, L.M., 2001, AJ, 121, 1676

Rebull, L. M., Wolff, S. C., Strom, S. E. & Makidon, R. B., 2002, AJ, 124, 546

Rebull, L. M., Wolff, S. C. & Strom, S. E., 2004, AJ, in press.

Royer, F., Grenier, S., Baylac, M.O., Gomez, A.E., & Zorec, J. 2002, A&A, 393,897

Scalo, J. 1998, in ASP Conf. Ser., Vol. 142, The Stellar Initial Mass function, ed. G. Gilmore & D. Howell (San Francisco: ASP)

Siess, L., Dufour, E. & Forestini, M. 2000, A&A, 358, 593

Siess, L., Livio, M., 1997, ApJ, 490, 785

Song, I., Zuckerman, B. & Bessell, M.S., 2003, ApJ, 599, 342

Song, I., Zuckerman, B. & Bessell, M.S., 2004, ApJ, 603, 804

Stassun, K.G., Ardila, D.R., Barsony, M., Basri, G. & Mathieu, R.D., 2004, AJ, submitted

Stassun, K.G., Mathieu, R.D., Mazeh, T. & Vrba, F.J., 1999, AJ, 117, 2941

Stassun, K.G. & Terndrup, D., 2003, PASP, 115, 505

Stauffer, J. R., 2001, in ASP Conf. Ser., Vol. 244, Young Stars Near Earth: Progress and Prospects, ed. R. Jayawardhana & T. Greene(San Francisco: ASP)

Stauffer, J. R., 1997, AJ, 479, 776

Stauffer, J. R., Caillault, J. P., Gaigé, M., Prosser, C. F. & Hartman, L. W.,1994, ApJS, 91, 625

Stelzer, B. & Neuhäuser, R., 2000, A&A, 361,581

Stelzer, B. & Neuhäuser, R., 2001, A&A, 372,117

Suchkov, A. A., Makarov, V. V. & Vogues, W., 2003, ApJ, 595, 1206

Tinker, J., Pinsonneatult, M. & Terndrup, D., 2002, AJ, 564,877

Torres, C.A.O., da Silva, L., Quast, G. & de la Reza, R., 2000, AJ, 120, 3

Torres, G., Guenther, E., Marschall, L., Neuhäuser, R., Latham, D. & Stefanik, R., 2003, ApJ, 125, 825

Weinberger, A. J., Becklin, E. E., Zuckerman, B. & Song, I., 2004, AJ, 127, 2246

Weinberger, A. J., Becklin, E. E. & Zuckerman, B., 2003, ApJ, 584, L33

Webb, R.A., 1999, ApJ, 512, L63

Webb, R.A., 2001, in ASP Conf. Ser., Vol. 244, Young Stars Near Earth: Progress and Prospects, ed. R. Jayawardhana & T. Greene(San Francisco: ASP)

Wolff, S. C., Strom, S. E. & Hillenbrand, L. A., 2004, ApJ, 601, 979

Wichmann, R., Bouvier, J., Allain, S. & Krautter, J., 1998, A&A, 330, 521

Zuckerman, B., Song, I., Bessell, M. & Webb, R., 2001a, ApJ, 562, L87

Zuckerman, B., Song, I. & Webb, R., 2001b, ApJ, 559, 388

Zuckerman, B. & Webb, R. 2000, ApJ, 535, 959
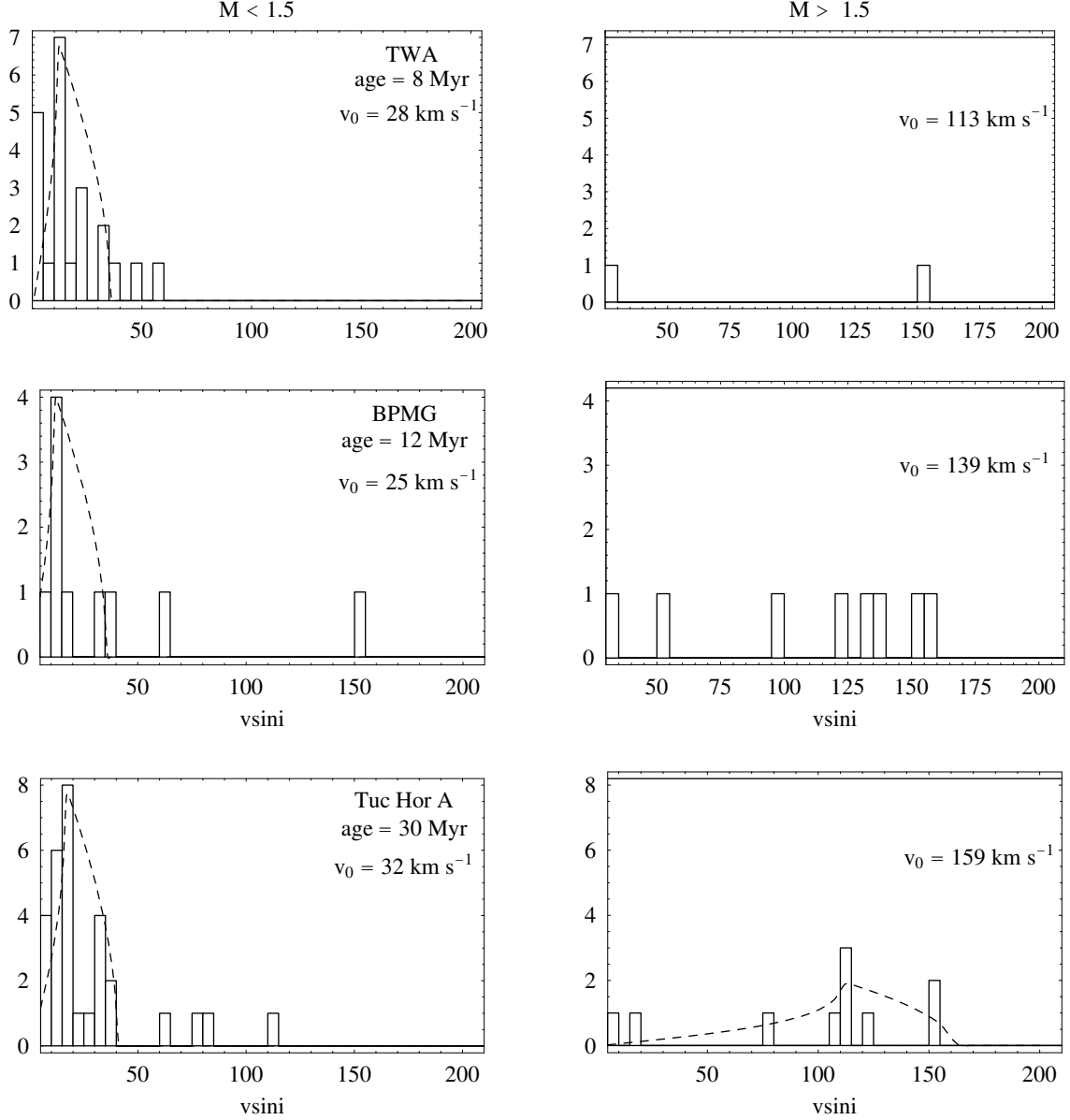
Fig. 1.— *vsini* distributions in $km\ s^{-1}$ for the three associations studied in this work. Left column correspond to masses less than $1.5 M_{\odot}$ and right column to masses greater or equal than $1.5 M_{\odot}$. Mean equatorial rotation velocities $v_0(eq)$ for LM and HM rotation modes corresponding to the fitting procedure (see text) and the ages for each association are indicated. We have taken $a = 5\ km\ s^{-1}$ except for the high mode of Tuc/HorA in which $a = 10\ km\ s^{-1}$
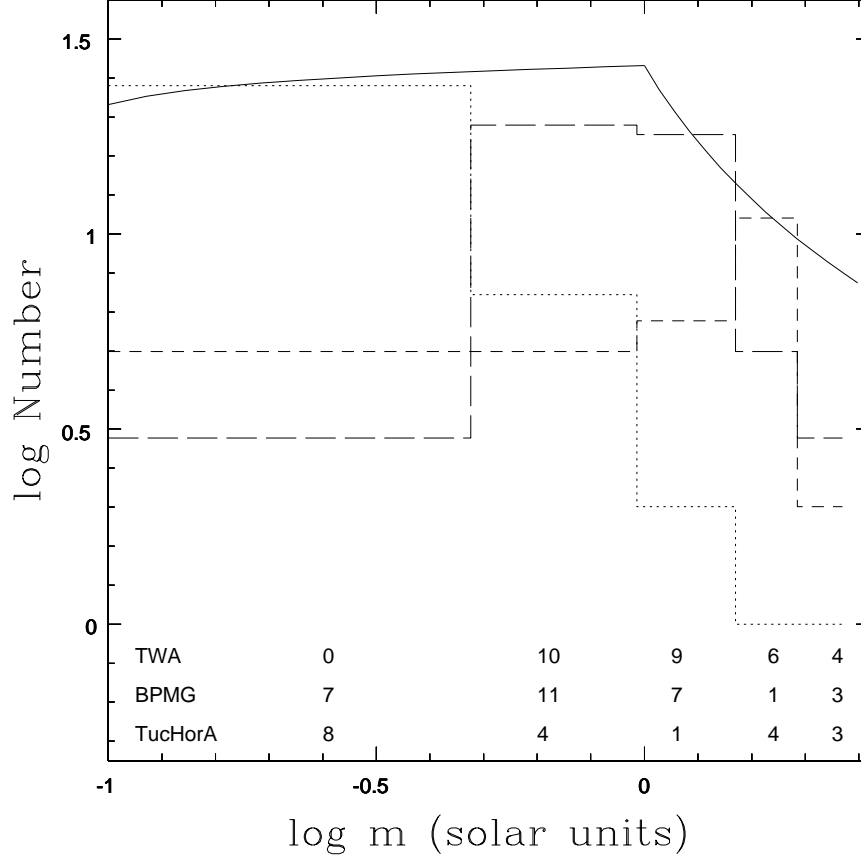
Fig. 2.— Comparison of mass distributions with the IMF. The dotted histogram correspond to TWA, long dashed histogram to BPMG and the short dashed for Tuc/HorA. Our two-segment power law are represented by a continuous line. The number of predicted stars for each association and mass intervals obtained from the differences between the IMF and observed distributions is indicated.
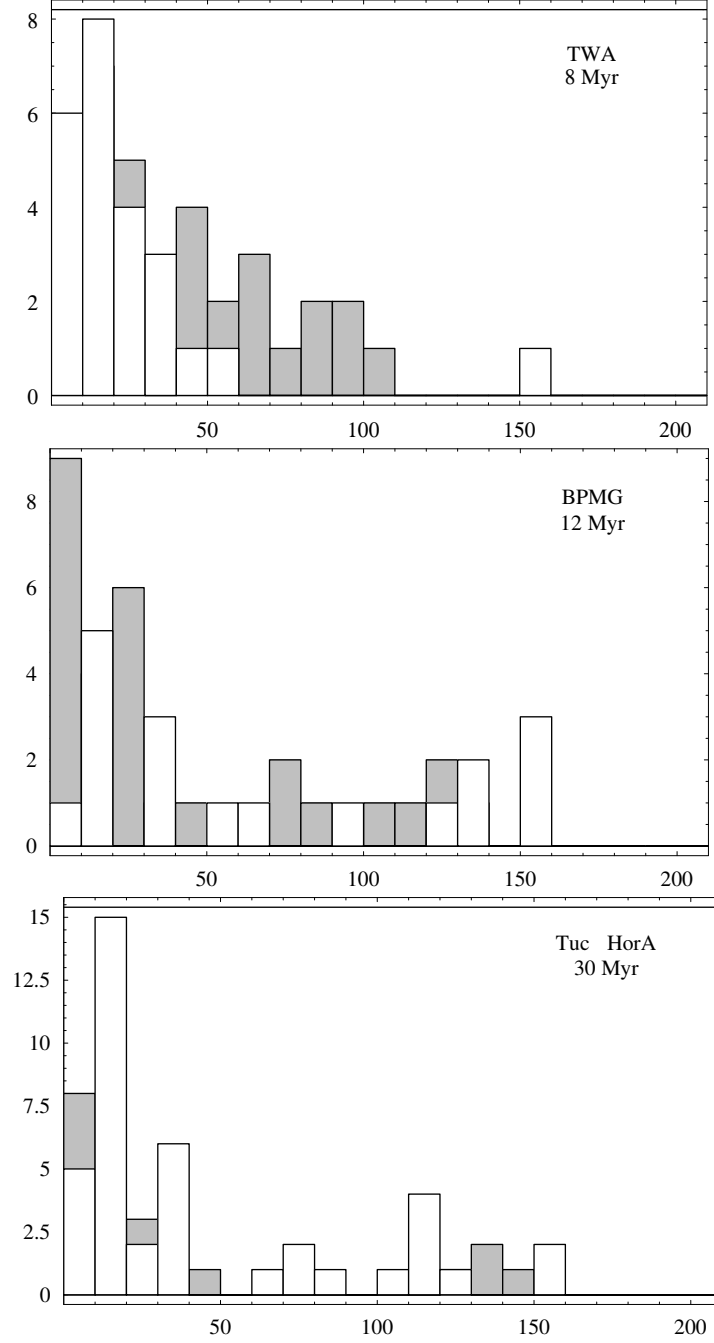
Fig. 3.— *vsini* distributions in $km\ s^{-1}$ of the LM and HM rotating modes. White and grey bars represent respectively observed and simulated values (see text)
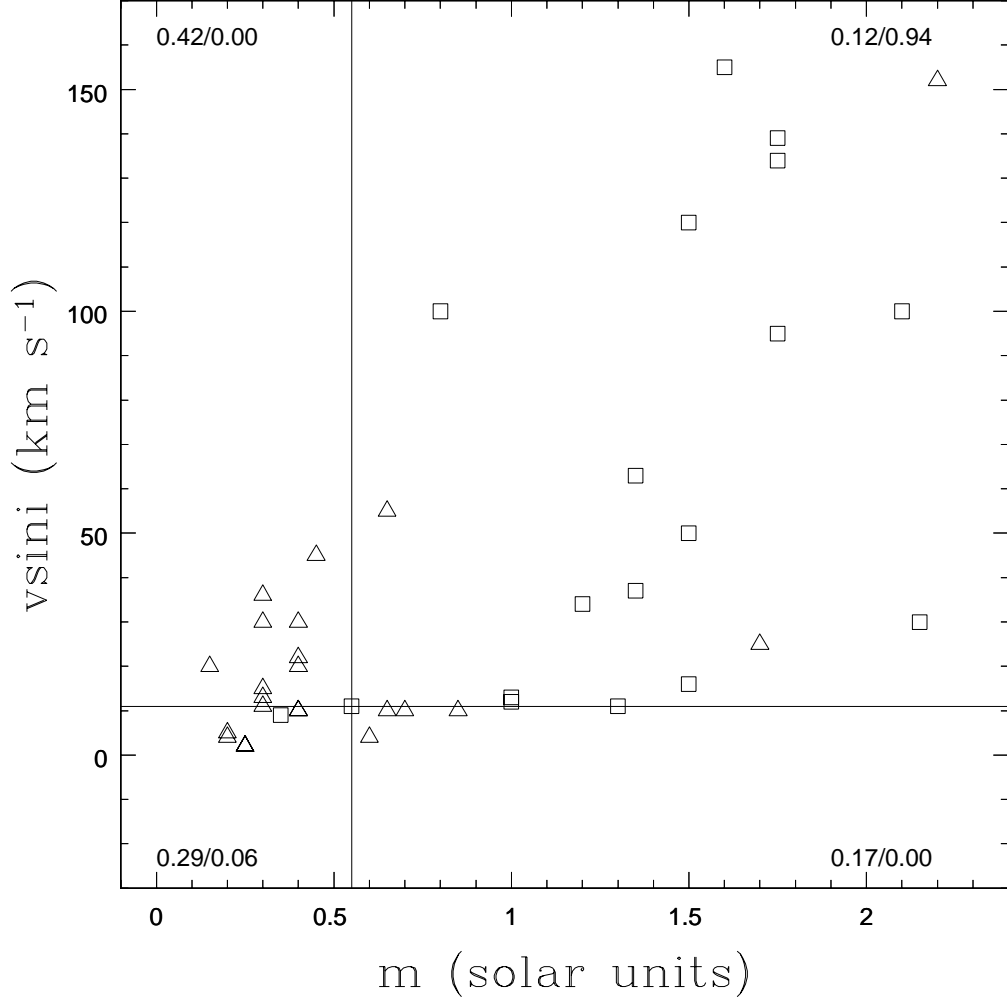
Fig. 4.— Two dimension K-S test applied to the mass-*vsini* distributions corresponding to the TWA and BPMG associations. The algorithm of Press et al.(1994) calculates the origin point whose quadrants maximizes the difference between fraction of triangles (TWA) and fraction of squares (BPMG). The maximum occurs in the upper-right quadrant. At this quadrant the smallest probability of null hypothesis is found.
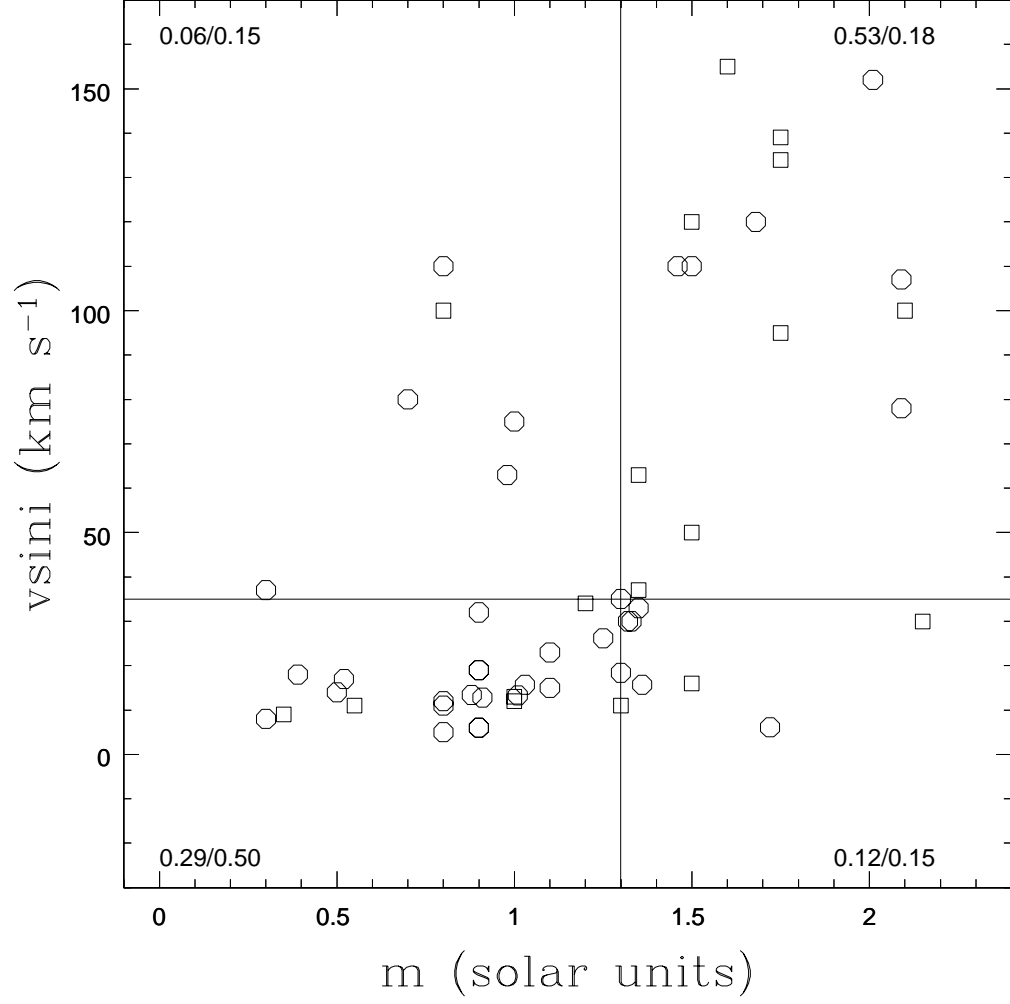
Fig. 5.— K-S test applied to BPMG (squares) and Tuc/HorA (polygons) associations. The same as in Figure 4, the maximum differences are found in the upper right quadrant.
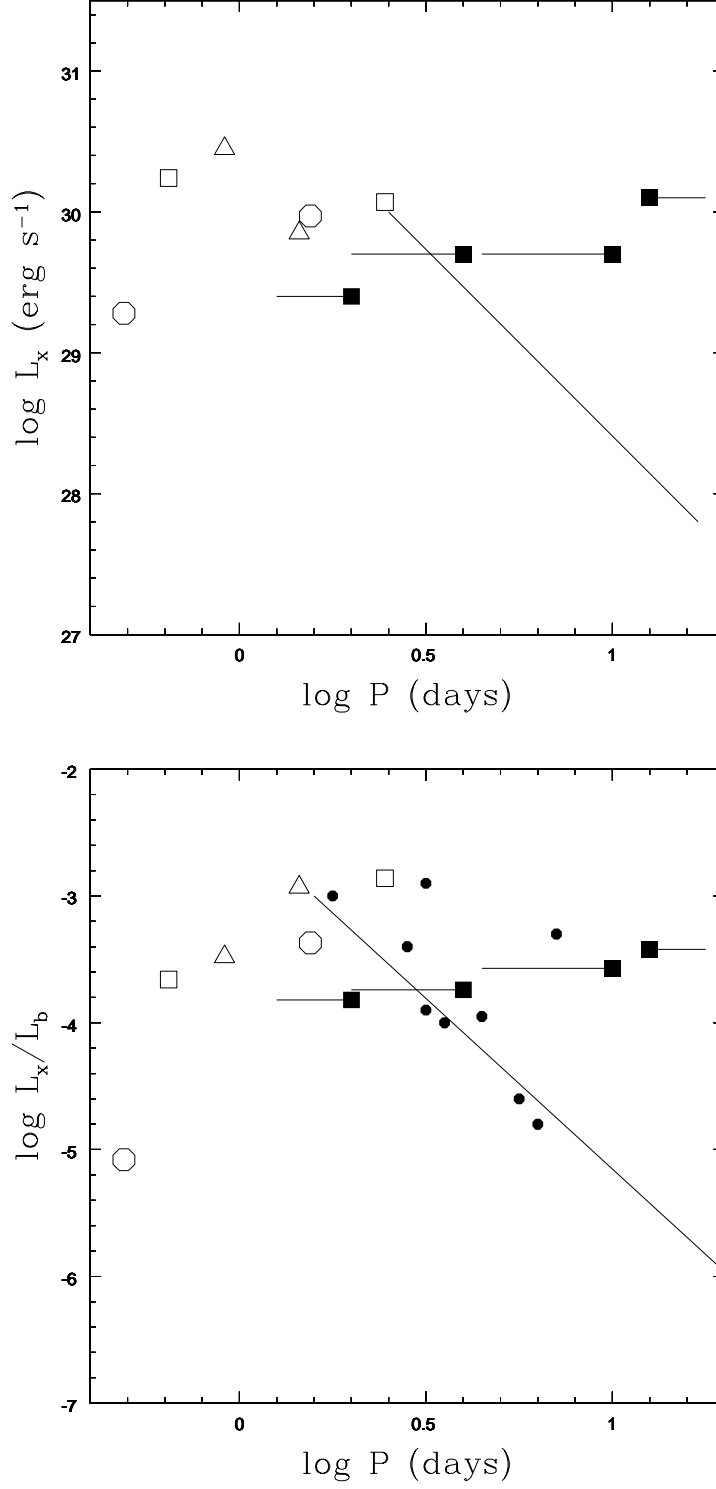
Fig. 6.— Schematic time evolution of mean L_x and $logL_x/L_b$ for both LM and HM rotating modes. Open symbols represent TWA (triangles), BPMG (squares) and Tuc/HorA (polygones). Filled squares corresponds to ONC data taken from Feigelson et al.(2003). In the bottom panel the filled circles are taken from Huélamo (2002) and represent 9 PTTS belonging to Lindroos systems.
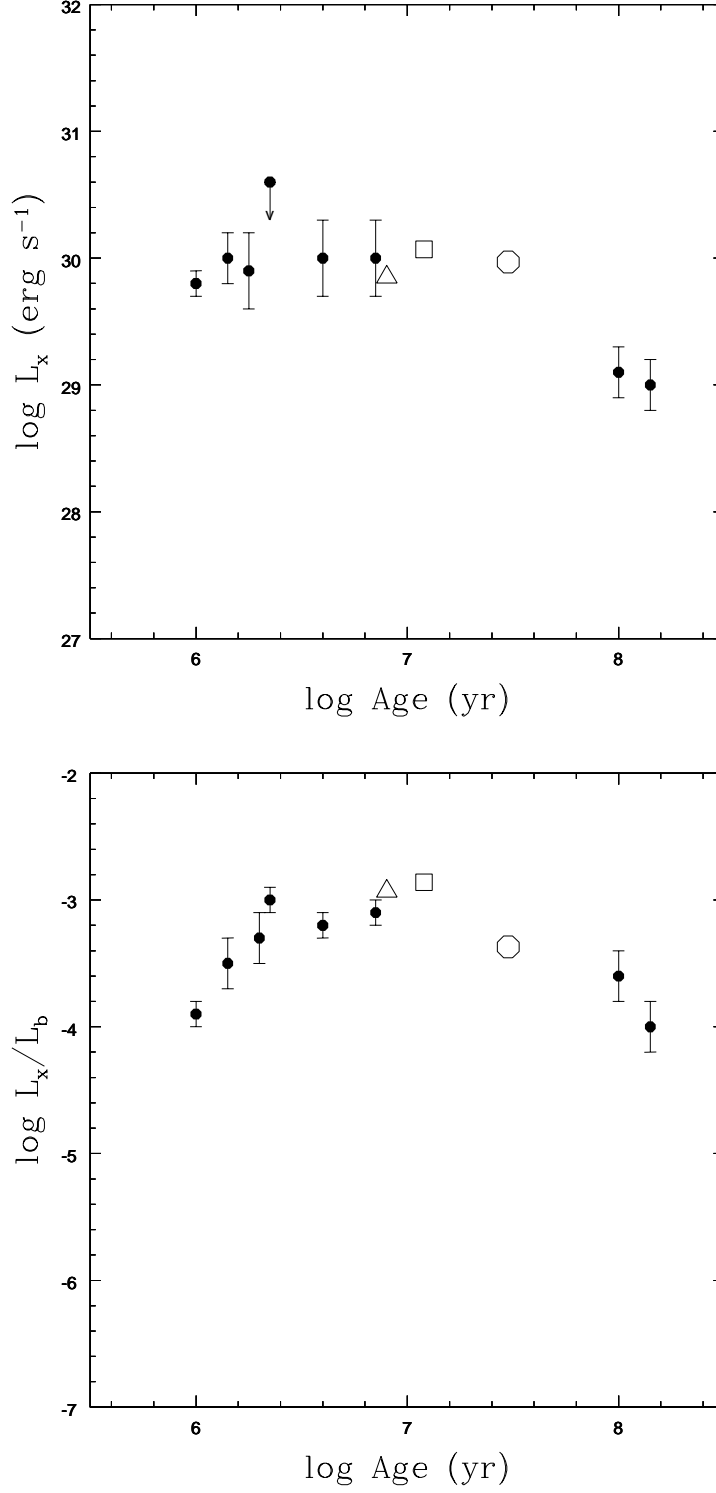
Fig. 7.— Mean values of the X-rays indicators as function of age for the lower rotating mode. Open symbols represent TWA (triangles), BPMG (squares) and Tuc/HorA (polygones). Filled circles taken from Flaccomio et al.(2003b) represent T Tauri stars (left side) and early MS stars (right side).
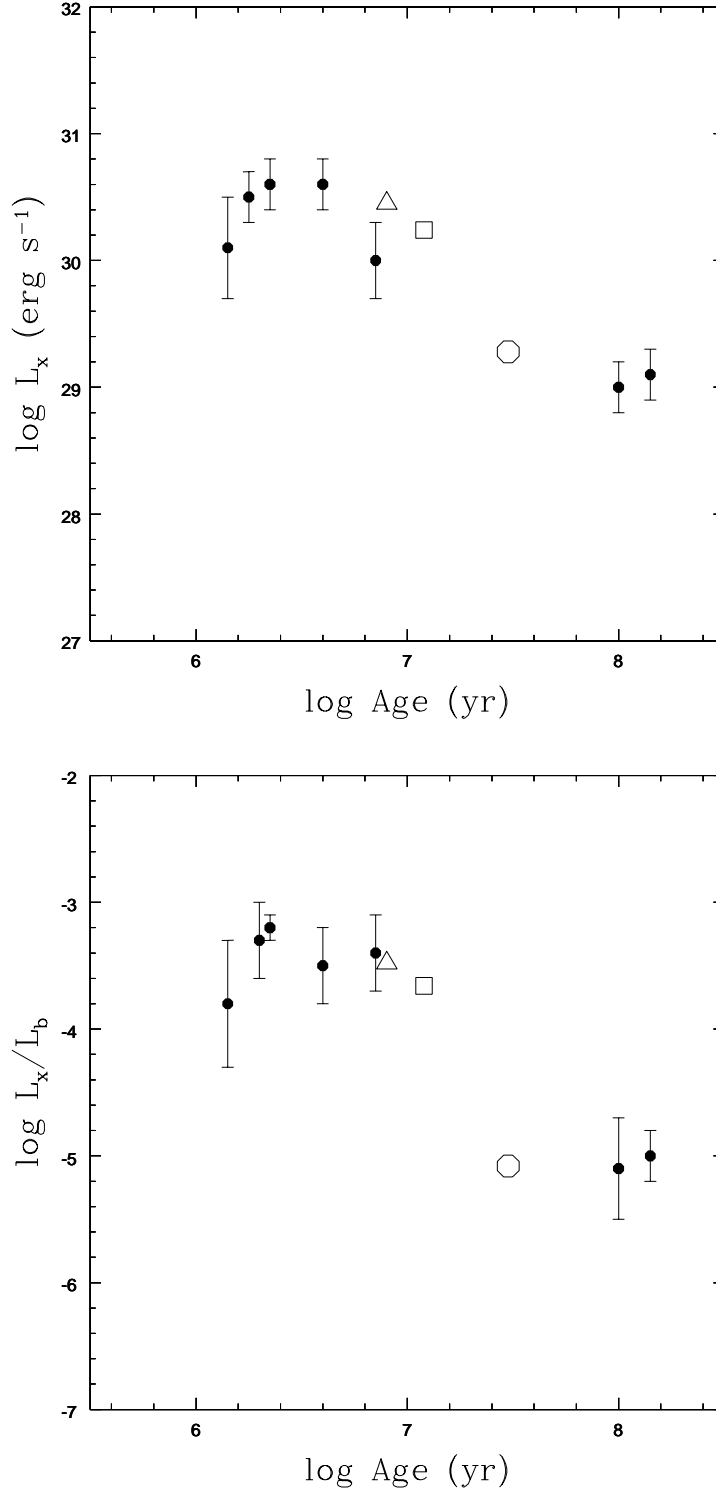
Fig. 8.— As in Figure 7 but for the high rotating mode.
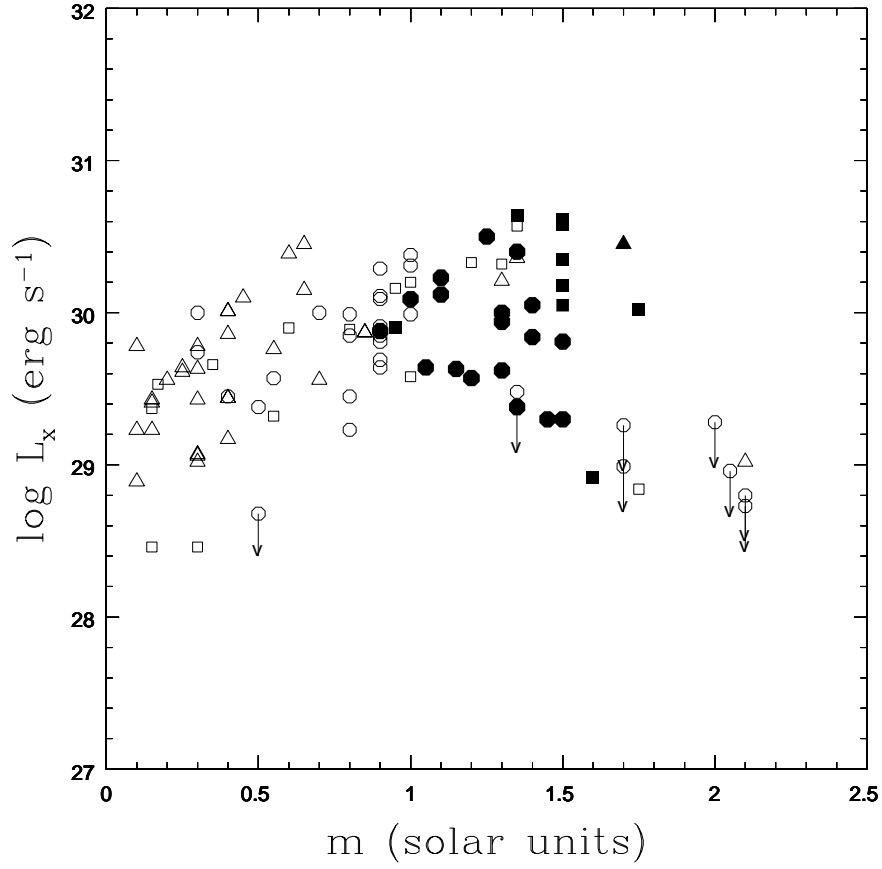
Fig. 9.— L_x *vs* stellar masses for the associations. The F and G stars are represented by black symbols. Upper limit values are represented with arrows.
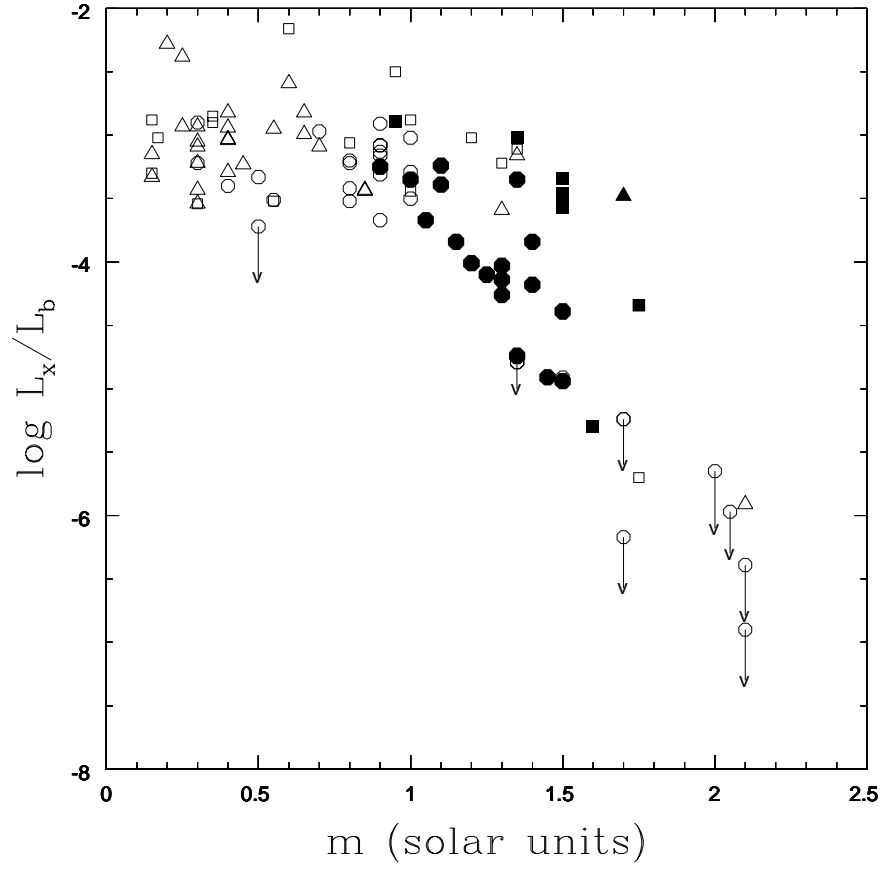
Fig. 10.— L_x/L_b vs stellar masses for the associations. The symbols are the same as in Figure 9.

Table 1. TWA

Name	ST	V	B-V	V-I_c	M	R	$vsini$	d	log L_x	log L_x/L_{bol}	Ref.
TWA Hya:TWA1	K7e	10.92	0.97	1.70	0.60	1.0	4	56.4	30.39	-2.59	1,7
CD-29° 8887A:TWA2A	M2e	11.07	1.48	2.24	0.30	0.70	13	43	29.43	-3.54	1,7
CD-29° 8887B:TWA2B	M2	...	...	2.80	0.15	0.6	...	43	29.43	...	1,2,7
Hen 3-600A:TWA3A	M3e	12.04	1.49	2.94	0.15	0.55	20	35	29.23	-3.33	1,7
Hen 3-600B:TWA3B	M3.5	13.70	...	3.60	≤0.1	≤0.5	...	35	29.23	...	1,2,7
HD 98800A:TWA4A	K4/K5	9.41	1.15	1.51	0.85	1.15	10	46.7	29.87	-3.43	1,7
HD 98800B:TWA4B	K7+M1	9.94	1.28	...	0.85	0.70	...	46.7	29.87	-3.44	1
CD-33° 7795A:TWA5A	M1.5	11.54	1.48	2.62	0.30	0.70	36	48	29.78	-3.05	1,2
CD-33° 7795B:TWA5B	M8.5	20.40	...	4.60	≤0.1	≤0.5	...	48	29.78	...	1,2
TYC 7183- 1477- 1:TWA6	K7	11.62	1.31	1.68	0.65	1.05	55	77	30.15	-2.82	1,2
TYC 7190- 2111- 1:TWA7	M1	11.65	1.46	2.44	0.25	0.70	2	38	29.64	-2.38	1,2,7
TWA 8A	M2	13.30	1.46	2.41	0.25	0.70	2	21	...	...	1,2,7
TWA 8B		...					5	21	...	...	1,2
CD-36° 7429A:TWA9A	K5	11.26	1.26	1.62	0.70	1.00	10	50.3	29.56	-3.09	1,2,7
CD-36° 7429B:TWA9B	M1	14.00	1.42	2.58	0.20	0.60	4	50.3	29.56	-2.28	1,2,7
GSC 07766-00743:TWA10	M2.5	12.96	1.43	2.47	0.25	0.80	2	57	29.61	-2.93	1,2,7
HR4796A:TWA11A	A0	5.78	0.00		2.10	1.65	152	67.1	29.02	-5.91	1,10
HR4796B:TWA11B	M2.5	13.30	...		0.30	0.75	...	67.1	29.02	-3.22	1,2
RX J1121.1-3845:TWA12	M2	12,85?	1.50	2.25	0.30	0.75	15	32	29.06	-2.93	1,2
RX J1121.3-3447N:TWA13A	M1e	11.46	1.44	1.97	0.40	0.80	10	38	29.44	-3.03	1,7
RX J1121.3-3447S:TWA13B	M2e	12.40	1.44	1.97	0.40	0.80	10	38	29.44	-3.04	1,7
1RXS J111325.1-452344:TWA14	M0	11.85	...	2.85	0.15	0.60	...	46	29.41	-3.15	1,2
1RXS J123420.1-481514:TWA15A	M1.15	13.51	...	2.16	0.40	0.80	22	119	30.01	-2.82	1,2

Table 1—Continued

Name	ST	V	B-V	V-I_c	M	R	*vsini*	d	log L_x	log L_x/L_{bol}	Ref.
1RXS J123420.1-481514:TWA15B	M2	14.00	...	2.19	0.40	0.80	30	119	30.01	...	1,2
1RXS J123456.1-453808:TWA16	M1.5	11.64	...	2.13	0.30	0.80	11	66	29.63	-3.43	1,2
1RXS J132046.5-461139:TWA17	K5	11.69	...	1.92	0.45	0.90	45	133	30.10	-3.23	1,2
1RXS J132137.0-442133:TWA18	M0.5	12.08	...	1.98	0.40	0.80	20	98	29.86	-3.29	1,2
HD102458:TWA19A	G5	9.14	0.70	0.70	1.70	2.40	25	104.0	30.45	-3.48	1,2
HD102458B:TWA19B	K7	11.06	...	1.69	0.65	1.05	10	104.0	30.45	-2.99	1,2
A2-146:TWA20	M2	13.40	...	2.30	0.30	0.70	30	50 g	29.07	-3.09	2
HD298936:TWA21	M1	9.79	1.00	...	1.30	1.50	...	69	30.21	-3.59	3
SSS 101726.7-535428:TWA22	M5	...	1.80	...	≤0.1	0.30	...	22	28.89	...	3
SSS 120727.4-324700:TWA23	M1	12.67	1.48	...	0.40	0.85	...	37	29.17	-2.94	3
GSC 08644-00802:TWA24	K3	10.26	0.95	...	1.35	1.55	...	95	30.36	-3.16	3
GSC 07760-00283:TWA25	M0	11.36	1.40	...	0.55	0.95	...	44	29.76	-2.95	3

Table 2.   BPMG

Name	ST	V	B-V	V-I_c	M	R	$vsini$	d	$\log L_x$	$\log L_x/L_{bol}$	Ref.
HR9	F2	6.19	...	0.46	1.60	2.20	155	39.10	28.92	-5.30	4
55 Eri	F0	5.22	...	0.34	1.75	1.80	95	29.80	30.02	-4.34	4
GJ 3305	M0.5	10.59	1.90		≤0.1	≤0.38	...	29.80	30.23	-2.49	4
HIP 23309	M0/1	10.01	...	1.79	0.55	0.90	11	26.30	29.32	-3.52	4
HD 35850	F7	6.30	...	0.62	1.50	2.20	50	26.80	30.35	-3.52	4
BetaPic	A3	3.85	...	0.20	1.75	1.70	139	19.30	...	...	4
AO Men	K6/7	9.77	...	1.34	1.00	1.25	13	38.50	30.20	-2.88	4
V343Nor	K0	8.14	...	0.93	1.30	1.70	11	39.80	30.32	-3.22	4
V343NorB	...	14.80	...	2.90	0.15	0.45	...	39.80	...	...	3
HR6070	A0	4.80	...	1.01	2.15	1.70	30	43.00	...	...	4
HD155555A	G5	7.21	...	0.81	1.35	1.80	37	31.40	30.64	-3.02	4
HD155555B	K0	8.08	...	1.09	1.20	1.30	34	31.40	30.33	-3.02	4
HD155555C	M4.5	12.71	...	2.69	0.17	0.50	...	31.40	29.53	-3.02	4
HD164249	F5	7.01	...	0.53	1.50	2.20	...	46.90	30.58	-3.48	4
HR6749	A5	5.67	...	0.26	1.80	1.80	...	43.90	...	...	4
HD172555	A7	4.78	...	0.20	1.75	1.70	134	29.20	28.84	-5.70	4
CD-64° 1208	K7	9.54	...	1.55	0.80	1.10	150	29.20	29.89	-3.06	4
PZ Tel	K0	8.25	...	0.85	1.35	1.85	63	49.70	30.57	-3.11	4
HR 7329	A0	5.05	...	0.04	2.10	1.65	150	47.70	...	...	4
HR7329B	M7/8	11.93	...	...	...	...	...	47.70	...	...	4
HD181327	F5.5	7.03	...	0.53	1.50	1.70	16	50.60	...	...	4
GJ799	M4.5e	11.02	...	2.90	0.15	0.70	...	10.20	29.37	-2.88	4
GJ803	M1e	8.81	...	2.10	0.35	0.75	9	9.90	29.66	-2.85	4

Table 2—Continued

Name	ST	V	B-V	V-I_c	M	R	$vsini$	d	$\log L_x$	$\log L_x/L_{bol}$	Ref.
HD199143	F8	7.34	...	0.62	1.50	2.20	120	47.70	30.61	-3.34	4
BD-17° 6128	K7/M0	10.60	...	1.30	1.00	1.25	12	47.70	29.58	-3.44	4
HD 14082 B	G2	7.75	0.62	...	1.50	1.30	...	34.00	30.05	-3.46	3
HD 14082	F8	6.99	0.52	...	1.50	1.10	...	39.40	30.18	-3.57	3
BD+30 397A	G9/K0	10.12	1.21	...	0.95	1.75	...	42.30	29.90	-2.89	3
BD+30 397B	K5/K6	12.44	1.40	...	0.60	1.70	...	42.30	29.90	-2.16	3
BD+05 378	G9/K0	10.37	1.22	...	0.95	1.75	...	40.50	30.16	-2.50	3
GJ 3322	M1/M2	11.50	1.50	...	0.35	1.65	...	32.10	29.60	-2.90	3
GJ 871.1A	M2	12.16	1.51	...	0.30	1.65	...	23.60	28.46	-3.54	3
GJ 871.1B	M3/M4	13.43	1.58	...	0.15	1.65	...	23.60	28.46	-3.30	3

Table 3.   Tuc/HorA

Name	ST	V	B-V	V-I_c	M	R	*vsini*	d	log L_x	log L_x/L_{bol}	Ref.
HD1466	F8	7.45	0.54	0.59	1.3	1.25	18	40.9	29.62	-4.14	5,6
HIP1910	M0	11.47	1.39	1.95	0.4	0.50	18	46.3	29.45	-3.4	5,6
HIP1993	K7	11.47	1.35	1.81	0.5	0.60	17	37.4	≤28.68	≤-3.72	5,6,8,9
HD2884	B9	4.38	-0.07	0.00	2.1	1.65	107	42.8	≤28.80	≤-6.39	5,6,8,9
HD2885	A2+A7	4.55	0.15?	0.25	1.7	1.50	6	52.8	≤28.99	≤-6.17	5,6,8,9
HD3003	A0	5.06	0.04	0.00	2.1	1.65	78	46.5	≤28.73	≤-6.90	5,6,8,9
HD3221	K4	9.63	1.05	1.38	0.8	0.80	110	45.9	29.99	-3.2	5,6
CPD-64120	K1e	10.29	0.86	1.01	0.9	0.95	32	59	30.09	-2.91	7
HD8558	G6	8.5	0.68	0.77	1.1	1.05	15	49	30.12	-3.39	7
HD9054	K2	9.07	0.91	1.01	0.9	0.95	6	37	29.81	-3.31	7
GSC8047-0232	K3	10.87	0.95	1.08	0.9	0.90	19	89	30.11	-3.08	7
HD12039	G4/G5	8.07	0.65	...	1.2	1.15	...	42.4	29.57	-4.01	3
CD-53386	K3e	11.02	0.96	1.12	0.9	0.90	19	117	30.29	-3.08	7
HD12894	F4	6.43	0.36	0.43	1.5	1.45	110	47	29.3	-4.94	7
HD13183	G5	8.63	0.65	0.76	1.1	1.05	23	50	30.23	-3.24	7
CD-60416	K5	10.68	1.16	1.43	0.8	0.80	12	45	29.85	-3.22	7
HD13246	F7	7.5	0.52	0.6	1.3	1.25	35	45	30.00	-4.26	7
GSC8056-0482	M3e	12.11	1.48	2.33	0.3	0.40	37	42	29.74	-2.90	7
GSC8491-1194	M3e	12.21	1.49	2.4	0.3	0.40	8	40	30.00	-3.22	7
CD-53544	K6e	10.21	1.26	1.6	0.7	0.70	80	40	30.00	-2.97	7
GSC8497-0995	K6e	10.97	1.23	1.48	0.8	0.75	5	48	29.23	-3.52	7
GSC8862-0019	K4e	11.67	1.04	1.25	0.9	0.85	6	98	29.85	-3.13	7
CD-65149	K2e	10.19	0.83	...	1.0	1.00	75	84	30.31	-3.02	7

Table 3—Continued

Name	ST	V	B-V	V-I_c	M	R	$vsini$	d	log L_x	log L_x/L_{bol}	Ref.
GSC84999-0304	M0e	12.09	1.25	1.54	0.8	0.75	11	77	29.45	-3.42	7
TYC 5882- 1169-1	K3/K4	10.17	1.01	...	0.9	0.95	...	51	30.35	-3.36	3
HD30051	F5	7.12	0.41	...	1.5	1.50	...	58.1	29.81	-4.39	3
HD35114	F7/F8	7.39	0.51	...	1.4	1.40	...	45.7	30.05	-3.84	3
TYC 7600- 516-1	K1	9.58	0.84	...	0.85	1.00	...	53	29.98	-3.25	3
TYC 7065- 0879-1	K4/K5	11.23	1.09	...	0.9	0.90	...	70	29.69	-3.25	3
HD40216	F7	7.46	0.49	...	1.4	1.40	...	54.3	29.84	-4.18	3
HD43989	F9	7.95	0.54	...	1.35	1.35	...	49.8	30.40	-3.35	3
HD44627	K1	9.13	0.86	...	1	1.00	...	45.5	29.99	-3.29	3
HD49855	G3	8.94	0.7	...	1.15	1.10	...	56.5	29.63	-3.84	3
HD55279	G7	10.11	0.96	...	0.9	1.00	...	64.1	29.88	-3.25	3
HD174429	K0	8.25	0.78	0.85	1	1.00	63	49.6	30.38	-3.5	5,6,8,9
HD177171	F7	5.16	0.53	0.63	1.25	1.20	26	52.4	30.50	-4.1	5,6,8,9
HD181296	A0	5.05	0.02	...	2.05	1.65	150	47.6	≤28.96	≤-5.97	5,6,8,9
HD181327	F5	7.03	0.48	0.53	1.35	1.35	16	50.6	≤29.38	≤-4.74	5,6,8,9
HD191869S	F6.5	7.93	0.49	0.54	?	1.35	33	65.3	29.48	-4.79	5,6,8,9
HD191869N	...	8.07	...	0.57	1.35	1.30	30	65.3	29.48	-4.79	5,6,8,9
HD200798	A5	6.69	0.24	0.28	1.7	1.50	120	66.4	≤29.26	≤-5.24	5,6,8,9
HD202917	G5	8.68	0.69	0.8	1	1.05	13	45.8	30.09	-3.35	5,6,8,9
HD202947	K0	8.91	0.85	1.05	0.9	0.95	13	46	29.91	-3.16	5,6,8,9
HIP107345	M1	11.62	1.4	1.83	0.5	0.60	14	42.3	29.38	-3.33	5,6,8,9
HD207575	F6	7.22	0.51	0.56	1.3	1.30	30	45.1	29.94	-4.03	5,6,8,9
HD207964	F3	5.9	0.39	0.46	1.5	1.45	110	46.5	29.30	-4.91	5,6,8,9

Table 3—Continued

Name	ST	V	B-V	V-I_c	M	R	$vsini$	d	log L_x	log L_x/L_{bol}	Ref.
PPM366328	K0	9.67	0.8	1	0.55	0.90	...	50	29.57	-3.51	5,6,8,9
HD222259S	G5/G8	8.49	0.78	0.78	1.05	1.05	16	46.2	29.64	-3.67	5,6,8,9
HD222259N	...	9.73	1.14	...	0.9	0.90	13	46.2	29.64	-3.67	5,6,8,9
HD224392	A1	5.01	0.06	0.06	2	1.60	152	48.7	≤29.28	≤-5.65	5,6,8,9

Note. — Probable and possible members of TWA (Table 1), BPMG (Table 2) and Tuc/Hor A (Table 3). Columns from left to right are: stellar name, spectral type, visual magnitude, $B-V$, $V-I_c$, stellar mass in solar units, stellar radius in solar units, observed projected rotational velocity in $km\ s^{-1}$, distance in pc (values with decimal correspond to Hipparcos values), X-ray luminosity L_x in $erg\ s^{-1}$, ratio of L_x/L_b where L_b is the bolometric luminosity. References: (1) Torres et al.(2003), (2) Reid (2003), (3) Song, Zuckerman & Bessell (2003,2004), (4) Zuckerman et al.(2001a), (5) Zuckerman & Webb (2000), (6) Zuckerman, Song & Webb (2001b), (7) Torres et al.(2000), (8) Stelzer & Neuhäuser (2000), (9) Stelzer & Neuhäuser (2001), (10) Royer et al.(2002)

Table 4.

Association	Age	$v_0(eq)$	$log < P >$	$log < L_x >$	$log < L_x/L_b >$	N
TWA	8	28/113	0.16/-0.04	29.85/30.45	-2.93/-3.48	31/2
BPMG	12	25/139	0.39/-0.19	30.07/30.24	-2.86/-3.66	19/13
Tuc/HorA	30	32/159	0.19/-0.31	29.97/29.28	-3.37/-5.08	41/8

Association	$< M >$	$< R >$	k^2_{conv}	k^2_{rad}	k^2_{total}	J/M
TWA	0.42/1.90	0.8/2.03	0.200/0.000	0.000/0.033	0.200/0.033	$3.1\times10^{16}/5.3\times10^{16}$
BPMG	0.67/1.68	1.20/1.79	0.183/0.000	0.015/0.043	0.198/0.043	$4.1\times10^{16}/7.4\times10^{16}$
Tuc/HorA	0.96/1.77	0.98/1.54	0.000/0.000	0.084/0.043	0.086/0.043	$1.9\times10^{16}/7.3\times10^{16}$

Note. — Mean characteristic values for low rotation / high rotation modes for the three associations. Columns in order are: for the upper table: association name, age in Myr, equatorial velocity in $km\ s^{-1}$, rotation period in days, X-ray luminosities in $erg\ s^{-1}$, ratio of luminosities and total number of stars considered in each case. In the lower table: association name, stellar mass in solar units, stellar radius in solar units, square of the convective radius of gyration, square of the radiative radius of gyration, square of the total radius of gyration and specific angular momentum in $cm^2\ s^{-1}$.